Scripta Materialia 277 (2026) 117238

Contents lists available at ScienceDirect

Scripta Materialia

journal homepage: www.journals.elsevier.com/scripta-materialia

Low-energy proton implantation reveals the incipience of hydrogen embrittlement in a martensitic steel

D.F.L. Borges [a,b], R.O. Silva [c], I.S.F. Carneiro [d], N.W.S. Morais [e], R.L. Sommer [f], N.R. Checca Huaman [f], P.J. Uggowitzer [d], E. Kozeschnik [g], M.B. Djukic [h], P.F.P. Fichtner [i], C.G. Schön [b], M.A. Tunes [d,*]

[a] Instituto Federal do Espírito Santo, Av. Vitória, 1729, 29040-780, Vitória, ES, Brazil
[b] Universidade de São Paulo Escola Politécnica, Department of Metallurgical and Materials Engineering, Av. Prof. Mello Moraes, 2463, São Paulo, 05508-030, SP, Brazil
[c] Instituto Brasileiro de Qualidade Nuclear, Rua do Mercado, 11, 20010-120, Rio de Janeiro, RJ, Brazil
[d] Department Metallurgy, Chair of Nonferrous Metallurgy, Montanuniversität Leoben, Franz-Josef-Strasse 18, 8700, Leoben, Steiermark, Austria
[e] Center of Science and Technology of Materials, Instituto de Pesquisas Energéticas e Nucleares - IPEN, Av. Prof. Lineu Prestes, 2242, 05508–000, São Paulo, SP, Brazil
[f] Centro Brasileiro de Pesquisas Físicas, Rua Xavier Sigaud, 150, 22290-180, Rio de Janeiro, RJ, Brazil
[g] Institute of Materials Science and Technology, TU Wien, Getreidemarkt 9, 1060, Vienna, Austria
[h] University of Belgrade Faculty of Mechanical Engineering, Kraljice Marije 16, Belgrade, 11120, Serbia
[i] Universidade Federal do Rio Grande do Sul Instituto de Física, Av. Bento Gonçalves, 9500 - PO Box 15051, 91501-970, Porto Alegre, RS, Brazil

ARTICLE INFO

Keywords:
Hydrogen embrittlement
Hydrogen damage
Proton implantation
22MnB5 steel

ABSTRACT

Hydrogen embrittlement (HE) remains a critical challenge in steels, particularly as hydrogen gains importance as a clean energy carrier. Direct microstructural evidence of HE mechanisms is difficult to obtain due to the high mobility of hydrogen and the instability of crack propagation. In this study, we introduce a controlled experimental approach using low-energy proton implantation to locally introduce hydrogen into 22MnB5 press hardened steel. This technique, adapted from prior investigations in silicon, confines hydrogen-induced effects to a well-defined depth, enabling focused nano-scale analysis by transmission electron microscopy. The results reveal the nucleation of hydrogen-stabilized nano-cavities aligned in one-dimensional rafts, which subsequently coalesce into nano-cracks within the martensitic matrix. These findings provide direct experimental insight into the incipience of HE, supporting the synergistic action of hydrogen-enhanced localized plasticity and hydrogen-enhanced decohesion. The proposed methodology offers a promising route to systematically investigate the onset of hydrogen embrittlement in metallurgy with nanoscale resolution.

Hydrogen is ubiquitous and easily incorporated into metallic microstructures, where it interacts and/or accumulates in site-specific regions [1,2], leading to degradation of mechanical properties through hydrogen embrittlement (HE) [3–9]. Engineering strategies traditionally focus on reducing hydrogen ingress or mitigating its impact through alloy design [1]. Although HE has been recognised as a problem for more than 150 years [9], hydrogen has recently gained importance as a clean energy carrier [10,11], making exposure of materials to hydrogen unavoidable and necessitating a clear understanding of its degradation effects [12]. Multiple HE mechanisms have been proposed, and no single mechanism is universally dominant [5]. Classical concepts include pressurisation of voids or pores by molecular hydrogen [1], hydride formation in susceptible metals [13,14], and synergistic operation of Hydrogen-Enhanced Localised Plasticity and Hydrogen-Enhanced Decohesion (HELP + HEDE) in steels [3,15]. Direct microstructural evidence remains challenging due to high hydrogen mobility and lack of *in situ* techniques to measure hydrogen and its effects at nano- and atomic-scales as a function of time [9].

In this work, we show that low-energy proton implantation allows the introduction of a localised hydrogen concentration in materials, thus enabling controlled observation of the incipience of hydrogen-related damage. Protons with energies below 100 keV dissipate their energy mainly through electronic stopping, avoiding displacement cascades and vacancy supersaturation typical of high-energy irradiation [16]. As previously demonstrated for crack nucleation studies in silicon [17] and further explored through implantation-induced platelet formation at high doses [18], this approach yields a confined implantation depth while keeping implantation-induced defects at minimal levels. Applying this method to 22MnB5 Press-Hardned Steel (PHS) – a martensitic steel containing substantial residual stresses and characteristic defect

* Corresponding author.
E-mail address: matheus.tunes@unileoben.ac.at (M.A. Tunes).

https://doi.org/10.1016/j.scriptamat.2026.117238
Received 10 December 2025; Received in revised form 29 January 2026; Accepted 16 February 2026
Available online 26 February 2026

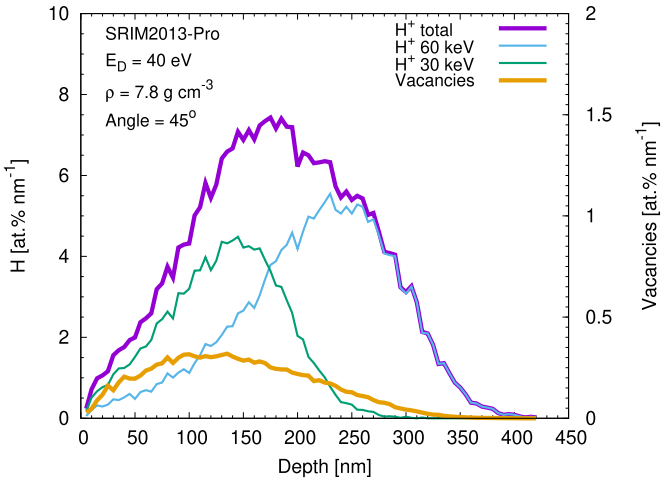

Fig. 1. Monte-Carlo calculation of implanted-hydrogen concentration and ion-beam-induced vacancies concentration profiles after the consecutive 30 and 60 keV proton implantations on the 22MnB5 PHS samples.

structures such as dislocations [19,20] – allows hydrogen-materials interactions to be investigated without significant radiation damage. Relevant overviews of hydrogen effects in martensitic steels were provided by Venezuela et al. [21,22], and a detailed metallurgical characterisation of 22MnB5 PHS has recently been reported by Liang et al. [23]. The nanoscale response to low-energy implantation is herein examined using focused ion beam preparation followed by transmission electron microscopy (TEM).

Strips with 1.4 × 25 × 150 mm were plasma-cut from an AlSi-coated 22MnB5 PHS automotive component, after which the coating was removed by grinding with #80 SiC paper. From these strips, 3 mm-diameter disks were produced by spark erosion using kerosene and a bronze tool, then ground to 0.4 mm thickness and further reduced to 0.1 mm using 200–1200# SiC papers. To minimise oxidation, the implantation surface was polished with a suspension containing 1 μm Al_2O_3, alkaline soap paste and distilled water, followed by mechanical polishing using 0.25 μm Al_2O_3 suspension. Proton implantation was performed at room temperature using a 500 kV High Voltage Engineering Europa B.V. (HVEE) ion implanter at the Ion Implantation Laboratory of the Federal University of Rio Grande do Sul (Brazil), with the beam incident at 45° relative to the surface normal. A dual-energy implantation was applied to broaden the hydrogen distribution: (i) $E = 60$ keV to a fluence of 8×10^{16} ions·cm^{-2} for 7 h 00 min, followed by (ii) $E = 30$ keV to 5×10^{16} ions·cm^{-2} for 4 h 40 min. Fig. 1 shows the resulting hydrogen and vacancy depth profiles as estimated using the SRIM2013-Pro Monte Carlo code [24], assuming a model 22MnB5 composition (at.%): C (1.15), Si (0.39), Mn (1.21), Cr (0.23), Ti (0.35), Fe (balance), with displacement energies of 40 eV for all elements [25] and 10 000 simulated ions.

Following low-energy proton implantation, the hydrogen-implanted microstructure of 22MnB5 PHS was examined *ex situ* by TEM. Electron-transparent lamellae were prepared by standard FIB lift-out procedures [26] using a TESCAN LYRA-3 dual-beam system with a Ga ion source. A protective Pt cap was deposited *in situ* prior to milling, and lamellae were thinned with decreasing probe currents (1 to 50 pA) before attachment to Cu lift-out grids. TEM analysis was performed on a JEOL 2100F (Schottky FEG, 200 kV) equipped with a 4k Gatan OneView camera. Specimen thicknesses were determined by EELS using a GIF Tridiem system, applying the logarithmic-ratio method [27], yielding $t = 26.2 \pm 4.3$ nm (see supplementary Information).

An electron microscopy characterisation of the 22MnB5 PHS before low-energy proton implantation is presented in Fig. 2A-B. The STEM-BF micrograph in Fig. 2A show lath martensite with micrometre grain-sizes, a typical microstructure for steels with a relatively low carbon content [28]. The high dislocation density is also representative and shown in Fig. 2B: these dislocations are associated with the intrinsic residual stresses of the martensite [19,20]. An important observation is the absence of ϵ-carbides. Such precipitates are reported to form even at low tempering temperatures and then serve as trapping sites for hydrogen, thereby influencing HE behaviour, *i.e.* increasing HE resistance [29].

The effects of low-energy proton implantation on the 22MnB5 PHS is shown in Fig. 2C–D. Similarly to Fig. 2A–B, the BFTEM micrograph in Fig. 2C shows a typical microstructure of lath martensite, characteristic of the investigated steel [23]. Particularly, one of the laths is parallel to the surface. Under-focus imaging reveals linear white-contrast features running approximately perpendicular to the surface, corresponding to nano-cavities aligned in a 1D raft. These ordered nano-cavities can be both voids and bubbles, but in the latter, may contain trapped hydrogen atoms and/or molecular hydrogen gas as the formation energy for dihydrogen in transition metals is in the order of ≈1 eV [30]. Their alignment cannot be attributed to any conventional microstructural feature, unlike the creep-induced rafting of γ' precipitates in nickel superalloys [31–33]. One possible origin of this 1D rafting in the 22MnB5 steel after proton implantation would be due to the interaction with some residual stress fields characteristic of quenched-in the martensite such as dislocations (see supplemental information). Rafting of precipitates in nickel superalloys is also associated with the behaviour of dislocations during creep [32]. Evans proposed that rafting and superlattice of voids and bubbles are formed in metals due to the diffusion of self-interstitial atoms, but in our case the interstitial diffusion of implanted hydrogen will be effectively reduced by an extraordinary number of traps [34–39] (*i.e.* the defects in the martensite). Several authors point out that this problem is not yet fully understood [13,40–42].

Analysis at deeper implantation depths show that these bubbles coalesce under the influence of implantation-induced black-spots (both visible in the micrographs Fig. 2C and D) and, further inside the sample, nano-cracks become visible. The latter can be noted in the higher-magnification underfocused BFTEM micrograph in Fig. 2D. Following the recent assessment of Harrison et al. on the self-organisation of nano-bubbles in gas-implanted W [42], the Fast-Fourier Transformation (FFT) shown as inset on Fig. 2D confirms the presence of 1D-rafting via the appearance of symmetric 60°/270° lobes.

Post-implantation analysis shown in Fig. 2C–D enabled the quantification of nano-cavities and nano-cracks generated by the two controlled low-energy proton implantations in the 22MnB5 PHS. The additional underfocused BFTEM micrographs in Fig. 3A–C were recorded after implantation at higher magnifications. They provide clear nanoscale evidence of nano-crack formation within the martensitic matrix. Applying a high-band-pass filter to the image in Fig. 3C and presenting the result in Fig. 3D, one can observe that the nano-cavities and nano-cracks are readily distinguishable both from themselves and the surrounding steel matrix. The histogram in Fig. 3E shows the distribution of nano-cavity diameters with the average estimated to be 1.20±0.02 nm whereas the histogram in Fig. 3F shows the distribution of nano-cracks with average length estimated to be 2.3±0.2 nm. The nano-cavities exhibit a regular, symmetrical size distribution around the average diameter, whereas the nano-cracks show an asymmetric distribution skewed toward sizes >2 nm and up to 11 nm, indicating that after formation from the coalescence of bubbles within the 1D-rafts, the nano-cracks initiate growth (and possibly) propagation within the microstructure of the 22MnB5 PHS. In summary, Figs. 2 and 3 show the qualitative and quantitative effects of low-energy proton implantation in 22MnB5 PHS.

These results clarify the early stages of HE in this steel, which proceed in three steps, schematically described in Fig. 4: (i) hydrogen enters the material and interacts with microstructural trapping sites [5,9,43], with quenched-in and implantation-induced vacancies promoting the formation of aligned nano-cavities (likely gas-filled); (ii) these cavities grow by short-range migration and coalescence driven by interstitial hydrogen diffusion and local stress fields; and (iii) continued coalescence

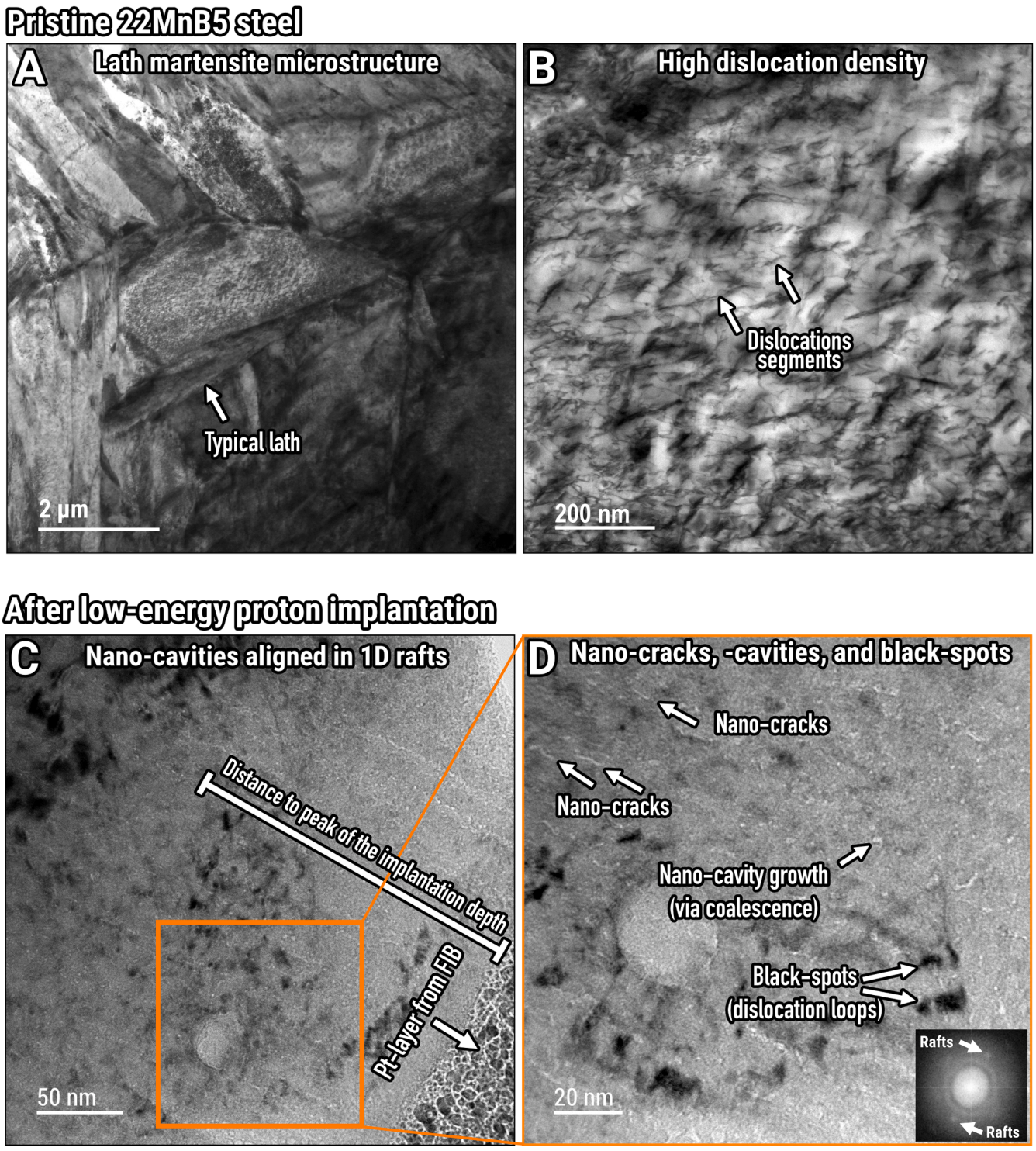

Fig. 2. The microstructure of the 22MnB5 PHS before low-energy proton implantation is shown in **A** and **B**, where both the typical lath martensite and high dislocation densities are noted, respectively. Upon implantation of monoatomic hydrogen in the matrix of this martensite steel with excess vacancies, **B** agglomeration nano-cavities in a 1D-raft alignment fashion is noted as particularly observed under BFTEM underfocused conditions. The underfocused BFTEM micrographs in **C** and **D** were taken at a higher magnification and indicate that nano-cavities within the 1D-rafts are able to coalesce and eventually this leads to the initiation of nano-cracks within the martensite as denoted by the white arrows (top-left). Note: the inset in **D** is an FFT of the BFTEM micrograph confirms the presence of 1D-rafting promoted by nano-cavities.

within the aligned raft produces nano-cracks that retain the original 1D arrangement.

The present study reveals that HE in 22MnB5 PHS may initiate through the nucleation, migration, and coalescence of nano-cavities, which can further evolve into nano-cracks within the martensitic matrix. The formation and propagation of hydrogen-assisted cracks – central topics in HE research since its first documentation in 1875 [9,44,45] – remain insufficiently understood. In the broader context of ion implantation of gaseous species, the formation of gas-filled bubbles has been extensively studied since the 1950s, with key contributions summarised by Thompson [46], Donnelly and Evans [47]. Self-organisation of bubbles into 1D rafts and 3D superlattices has also been reported across

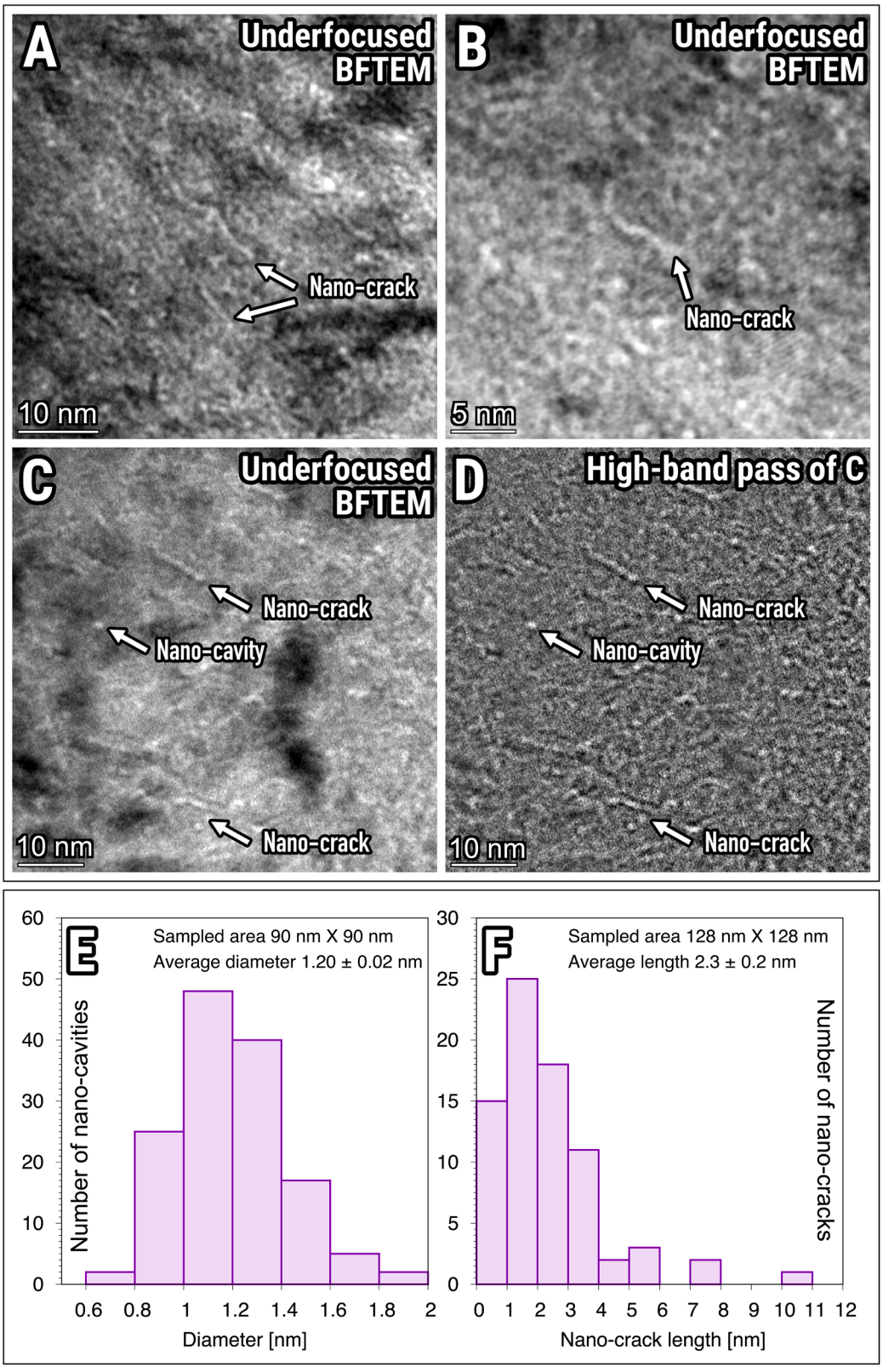

Fig. 3. BFTEM underfocused micrographs taken at higher-magnifications unequivocally shows in **A-C** the presence of nano-cracks in the 22MnB5 PHS as a result of low-energy proton implantation. The image in **D** shows a high-band pass filtered micrograph processed from **C** where nano-cavities and -cracks are clearly distinguishable from the martensite matrix. The histogram in **E** shows the average diameter of nano-cavities whereas the histogram in **F** shows the average length of nano-cracks. Low-energy proton implantation in controlled conditions leads to the formation of nano-cracks after nucleation, growth and coalescence of nano-cavities in the martensite of the 22MnB5 PHS.

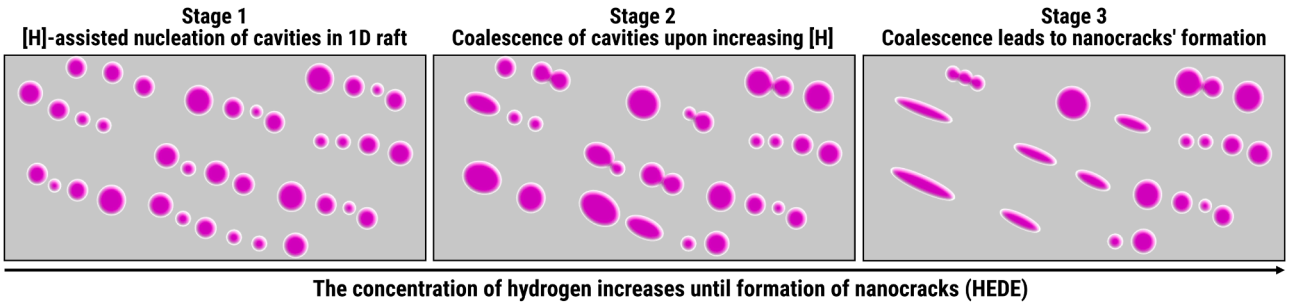

Fig. 4. Proposed mechanism to explain the incipience of HE in the 22MnB5 steel subjected to low-energy proton implantation.

various metals, alloys, and implantation conditions [40–42,48,49], particularly for inert gases such as helium due to their relevance in nuclear materials research [42,50–52]. Nano-cavities produced during ion implantation arise from vacancy formation and clustering, subsequently evolving into bubbles when gaseous species are trapped. Bubbles stabilise when vacancy and interstitial gas fluxes reach equilibrium, and grow or shrink if this balance is disturbed. Although bubble migration and coalescence are widely regarded as the dominant coarsening routes [47,53], the emergence of nano-cracks within a 1D raft – as observed here – constitutes a new result not previously reported for the experimental conditions and methodology.

To show that the observed nano-cracks arise directly from low-energy proton implantation and represent the onset of HE in the 22MnB5 PHS, it is necessary to recall key features of its shear martensitic microstructure. This martensite forms during cooling below the martensite start temperature through a coordinated lattice shear that produces lath or plate morphologies [20]. Such a transformation generates high dislocation densities [20] (as in Fig. 2B) and introduces non-equilibrium vacancies [54].

Once inside the matrix, hydrogen primarily interacts with both the pre-existing defects (dislocation segments) inherent to the martensitic matrix and its non-equilibrium population of vacancies. As the onset of HE in this steel under the studied conditions is linked – as demonstrated experimentally – to the formation and growth of nano-cavities and evolution into nano-cracks, the population of vacancies is a key parameter. Due to the martensite transformation, the non-equilibrium population of retained vacancies in the steel was previously estimated to be in the order of 1.0×10^{-4} at.% [54,55]. The low-energy proton implantation also induces the formation of an irradiation-induced population of vacancies – as shown in Fig. 1 – which peaks at around 1.5 at.% (≈100 nm) and with an average concentration around of 4.3×10^{-2} at.% for the whole implanted depth. Thus, the population of implantation-induced vacancies is about two orders of magnitude higher than that of quenched-in vacancies from shear martensite transformation, however, the distribution of irradiation-induced vacancies is asymmetric and concentrated in the forward implanted region, so that our present experimental approach to HE is able to introduce hydrogen in regions subject to the natural distribution of excess vacancies. In addition, the low implantation energy and low ion mass (in fact H^+ is the lowest possible mass for an ion) character of our experiments, yields that the total vacancy population generated due to the proton implantation remains far below the typically generated in ion implantations simulating nuclear environments [42,47].

In steels, the interaction between hydrogen and vacancies has a binding energy of around 0.6 eV [56], which is higher than both the binding energy between hydrogen and common steels' substitutional and interstitial solute atoms (≈ 0.1 eV [56]) and also the steel grain-boundaries (≤ 0.4 eV [57]). In this way, vacancies are not the preferable site by which hydrogen can get trapped (trapped hydrogen does not cause HE). However, the martensitic matrix has an intrinsic high-level of pre-existing defects such as dislocation segments, thus it is reasonable to assume – given Oriani's theory [35] developed upon the experimental data from Darken and Smith [34] and recently refined by several authors [36–39] – that the diffusion of implanted hydrogen will be significantly reduced as a high-number of dislocations act as extraordinary sites that promotes hydrogen trapping. A parallel is here noteworthy: interestingly, hydrogen diffusion in proton-implanted silicon – the motivation for our study – was also confirmed to be hindered by the presence of impurities and defects [58]. From these arguments, hydrogen is implanted in the 22MnB5 PHS and it will be prone to locally (*i.e.* at the short-range) interact with both defects of the martensite and the total population of non-equilibrium vacancies. Therefore, the observation of nano-cavities in a 1D raft fashion is intrinsically related with the existing population of defects (giving rise to regions with high strain) of the martensite and the ability of hydrogen to bind with excess vacancies given the limited mobility promoted by the existing martensite dislocations. The martensite full of defects also limits the movement of nano-cavities, thus coalescence takes place within the 1D rafts and among the nearest cavities: the implantation has been carried out at room temperature, therefore, no long-range movement of either vacancies or nano-cavities is expected to take place in this steel [53], yet the breakthrough observation of nano-cracks in the post-implanted specimens. As the low-energy proton implantation barely dislocate substitutional atoms from their lattice positions (*i.e.*, the setup does not cause severe radiation damage), we can reasonably assume that there is no significant irradiation-driven interstitial diffusion, therefore, the only actor in this metallurgical system that is driving nano-cavities formation and grow towards nano-cracks is – *de facto* – hydrogen.

Our work reveals that the phenomenon of HE in martensitic steels may initiate with the interaction between the implanted hydrogen with a population of non-equilibrium vacancies (in the range from 10^{-2} to 10^{-4} at.%), which is permitted given the lower hydrogen diffusivities due to pre-existing dislocations: a characteristic of the shear martensite [20]. Guedes-Oudriss-Feaugas et al. showed that elastic distortions in martensitic steels have little influence on hydrogen solubility, whereas the non-equilibrium vacancy population significantly enhances it [55]. Consistent with their findings, our low-energy proton implantation and post-implantation TEM analysis provide direct evidence that this vacancy-assisted hydrogen uptake drives HE through the nucleation, growth, migration, and coalescence of nano-cavities leading to crack formation.

A final note should be added regarding the initiation of HE in martensitic steels, as revealed by our recent research findings. This is related with the fundamental understanding of HE mechanisms in metallurgy. HELP (hydrogen interacts with dislocations and lowers the barriers for their movement) manifests in materials at low-hydrogen concentrations whereas HEDE (hydrogen weakens atomic bonding in lattice planes) operates in high-hydrogen concentrations. In between, as proposed by Djukic et al. [5], there exists a critical hydrogen concentration (C_H) that regulates the manifestation of either HELP or HEDE. Currently, the accurate estimation of C_H constitutes one of the major challenges for modern metallurgy giving the limitations on quantitatively measuring hydro-

gen concentrations in materials at the nano-scale [9]. HELP proposes that hydrogen accelerates ductile fracture by softening microstructural sites through interactions with dislocations [5,9,59,60]. Hydrogen is attracted to dislocation cores and surrounding elastic fields, increasing the dislocation mobility and leading to the formation of micro-voids, ultimately resulting in accelerated cracking. HEDE proposes that high levels of interstitial hydrogen at trapping sites cause atomic decohesion and crack initiation, leading to catastrophic brittle failure [5,9,60]. This process is thought to occur through a charge transfer between the hydrogen fundamental electron-orbital and the conduction band of transition metals, reducing the metal lattice's cohesive strength due to electric repulsion [61,62].

Which HE mechanism operates in the 22MnB5 PHS when hydrogen is implanted with low-energy proton beams at room temperature? We cannot estimate how much hydrogen is retained in the steel matrix after implantation, giving its high mobility even at room temperature, but we know with high-accuracy the concentration of hydrogen as a function of depth that has been implanted in the samples. This is shown in Fig. 1. The average hydrogen concentration on the implanted depth is between 1-2 at.%. As noted earlier, 22MnB5 PHS contains high densities of dislocations and non-equilibrium vacancies arising from both ion implantation and the shear-martensitic transformation. Our results showed that the combined presence of these defects promoted the nucleation of nano-cavities in a 1D rafting arrangement. The formation of nano-cavities itself requires the agglomeration of vacancies and incorporation of hydrogen atoms: as lately reviewed by Sugita et al. [63], Positron Annihilation Lifetime Spectroscopy (PALS) measurements confirmed the formation of stable hydrogen-vacancy clusters (pre-cavitation) in hydrogen-charged martensitic steels, corroborating our findings. In this way, our work shows for the first time that nano-cracks form due to this synergistic action of hydrogen interactions with elastic fields of pre-existing dislocations and excess vacancies: when hydrogen diffusivity is hindered by the elastic field of dislocations, hydrogen-vacancy clusters form, evolve to nano-cavities yielding nano-cracks formation. This suggests that the idea proposed by Djukic et al. [5] on the synergistic action of HELP + HEDE is the most appropriate HE mechanism governing the formation of nano-cracks: the presence of dislocations within the martensite (enhanced plasticity, HELP) mediate the formation of an ordered array of nano-cavities that upon nucleation and growth results in nano-cracks (decohesion, HEDE).

It is worth noting that this interpretation is consistent with the Hydrogen Enhanced Strain-Induced Vacancies (HESIV) mechanism [9,60,64–66]. In this concept, hydrogen is understood to increase the concentration of strain-induced vacancies, a phenomenon partially supported by PALS measurements [63]. The externally implanted vacancies in the present study therefore behave analogously to an increased population of strain-induced vacancies, facilitating cavity formation and subsequent cracking. In martensitic steels, however, the high density of pre-existing dislocations implies that HELP is likely to precede HESIV, thereby reducing hydrogen mobility and enabling the formation of hydrogen–vacancy clusters, ultimately evolving to nano-cracking, imaged by our work on the 22MnB5 PHS for the first time. Therefore, these remarks are in accordance with the unified HELP + HEDE model [5], which states that at the lower hydrogen concentrations and stress conditions, the possible simultaneous activity of plasticity-mediated HE mechanisms (HELP and HESIV) precedes nano-cracking due to HEDE dominance [8,9,15].

We presented a methodology for probing HE based on controlled low-energy proton implantation in a martensitic steel. Hydrogen was implanted in the steel with minimal radiation damage. TEM analysis revealed the formation of 1D rafts of nano-cavities that evolved into nano-cracks, providing insight into the underlying HE mechanism: a synergistic combination of HELP + HEDE. The influence of the inherent residual stresses of the martensite in the formation of the 1D raft of nano-cavities is a topic for further research. To assess the broader applicability of this approach for nanoscale HE studies, further work employing varied implantation energies, temperatures, and material systems is herein identified as necessary.

CRediT authorship contribution statement

D.F.L. Borges: Writing – review & editing, Methodology, Investigation, Formal analysis, Data curation; **R.O. Silva:** Investigation; **I.S.F. Carneiro:** Investigation, Formal analysis, Data curation; **N.W.S. Morais:** Investigation, Formal analysis; **R.L. Sommer:** Writing – review & editing, Supervision, Resources, Methodology, Investigation; **N.R. Checca Huaman:** Writing – review & editing, Visualization, Methodology, Investigation, Formal analysis, Data curation; **P.J. Uggowitzer:** Writing – review & editing, Supervision, Methodology, Investigation, Formal analysis; **E. Kozeschnik:** Writing – review & editing, Validation, Supervision, Investigation; **M.B. Djukic:** Writing – review & editing, Visualization, Validation, Supervision, Investigation, Formal analysis; **P.F.P. Fichtner:** Writing – review & editing, Visualization, Validation, Supervision, Resources, Methodology, Investigation, Formal analysis, Data curation; **C.G. Schön:** Writing – review & editing, Visualization, Validation, Supervision, Resources, Methodology, Investigation, Formal analysis, Conceptualization; **M.A. Tunes:** Writing – review & editing, Writing – original draft, Visualization, Validation, Supervision, Resources, Methodology, Investigation, Funding acquisition, Formal analysis, Conceptualization.

Data availability

The raw and processed data collected for the realisation of this research/manuscript can be found in the permanent repository: D.F.L. Borges et al. Data for: Low-energy proton implantation reveals the incipience of hydrogen embrittlement in a martensitic steel, Mendeley Data, V1, 2026. 10.17632/n37z7ztfm3.1

Declaration of competing interest

The authors declare that they have no known competing financial interests or personal relationships that could have appeared to influence the work reported in this paper.

Acknowledgments

MAT would like to thank the Austrian Research Promotion Agency (FFG) for funding provided to the project HydronVision (FFG No. 928330). HydronVision is funded by both the *Fonds Zukunft Österreich* and the FFG (www.ffg.at). The FFG is the central national funding organisation and strengthens Austria's innovative power. CGS acknowledges the financial assistance of the Conselho Nacional de Desenvolvimento Científico e Tecnológico (CNPq, Brasília-DF, Brazil) under grants 307627/2021-7 and 308959/2024-3. NRCH acknowledges the financial of the FAPERJ under grant E-26/210.370/2022. MAT and ISFC would like to thank Dipl.-Ing. Dr.mont. Thomas Kremmer (MUL) for his assistance with TEM sample preparation.

Supplementary material

Supplementary material associated with this article can be found in the online version at 10.1016/j.scriptamat.2026.117238.

References

[1] R. Gibala, R.F. Hehemann (Eds.), Hydrogen embrittlement and stress corrosion cracking, American Society for Metals, Metals Park-OH, Metals Park-OH, 1984. https://doi.org/10.3403/30219195

[2] Q. Li, H. Ghadiani, V. Jalilvand, T. Alam, Z. Farhat, M.A. Islam, Hydrogen impact: a review on diffusibility, embrittlement mechanisms, and characterization, Materials 17 (4) (2024). https://doi.org/10.3390/ma17040965

[3] M.B. Djukic, V. Sijacki Zeravcic, A. Sedmak, B. Rajicic, Hydrogen damage of steels: a case study and hydrogen embrittlement model, Eng. Failure Anal. 58 (2015). https://doi.org/10.1016/j.engfeilanal.2015.05.017

[4] M.B. Djukic, G.M. Bakic, V.S. Zeravcic, A. Sedmak, B. Rajicic, Hydrogen embrittlement of industrial components: prediction, prevention, and models, Corrosion 72 (7) (2016) 943–961. https://doi.org/10.5006/1958

[5] M.B. Djukic, G.M. Bakic, V.S. Zeravcic, A. Sedmak, B. Rajicic, The synergistic action and interplay of hydrogen embrittlement mechanisms in steels and iron: localized plasticity and decohesion, Eng. Fract. Mech. 216 (2019) 106528. https://doi.org/10.1016/j.engfracmech.2019.106528

[6] M.B. Djukic, Hydrogen embrittlement and material selection - prof. milos B. Djukic - mission hydrogen — youtube.com, 2023, https://www.youtube.com/watch?v=EpDTc1s5lVY. [Accessed 17-03-2024].

[7] H. Yu, A. Diaz, X. Lu, B. Sun, Y. Ding, M. Koyama, J. He, X. Zhou, A. Oudriss, X. Feaugas, Z. Zhang, Hydrogen embrittlement as a conspicuous material challenge-comprehensive review and future directions, Chem. Rev. 124 (10) (2024) 6271–6392. https://doi.org/10.1021/acs.chemrev.3c00624

[8] X. Li, J. Zhang, Y. Cui, M.B. Djukic, H. Feng, Y. Wang, Review of the hydrogen embrittlement and interactions between hydrogen and microstructural interfaces in metallic alloys: grain boundary, twin boundary, and nano-precipitate, Int. J. Hydrogen Energy 72 (2024) 74–109. https://doi.org/10.1016/j.ijhydene.2024.05.257

[9] M.A. Tunes, P. Uggowitzer, P. Dumitraschkewitz, P. Willenshofer, S. Samberger, F.C. da Silva, C.G. Schön, T.M. Kremmer, H. Antrekowitsch, M.B. Djukic, S. Pogatscher, Limitations of hydrogen detection after 150 years of research on hydrogen embrittlement, Adv. Eng. Mater. 26 (2024) 2400776. https://doi.org/10.1002/adem.202400776

[10] J. Hoschke, M.F.W. Chowdhury, J. Venezuela, A. Atrens, A review of hydrogen embrittlement in gas transmission pipeline steels, Corros. Rev. 41 (3) (2023) 277–317. https://doi.org/10.1515/corrrev-2022-0052

[11] M.F.W. Chowdhury, C. Tapia-Bastidas, V, J. Hoschke, J. Venezuela, A. Atrens, A review of influence of hydrogen on fracture toughness and mechanical properties of gas transmission pipeline steels, Int. J. Hydrogen Energy 102 (2025) 181–221. https://doi.org/10.1016/j.ijhydene.2025.01.018

[12] M.A. Kappes, T. Perez, Hydrogen blending in existing natural gas transmission pipelines: a review of hydrogen embrittlement, governing codes, and life prediction methods, Corros. Rev. 41 (3) (2023) 319–347. https://doi.org/10.1515/corrrev-2022-0083

[13] M.A. Tunes, R.W. Harrison, G. Greaves, J.A. Hinks, S.E. Donnelly, Effect of he implantation on the microstructure of zircaloy-4 studied using in situ TEM, J. Nucl. Mater. 493 (2017) 230–238. https://doi.org/10.1016/j.jnucmat.2017.06.012

[14] M.A. Tunes, C.M. Silva, P.D. Edmondson, Site specific dependencies of hydrogen concentrations in zirconium hydrides, Scr. Mater. 158 (2019) 136–140. https://doi.org/10.1016/j.scriptamat.2018.08.044

[15] H.W. Lee, M.B. Djukic, C. Basaran, Modeling fatigue life and hydrogen embrittlement of bcc steel with unified mechanics theory, Int. J. Hydrogen Energy 48 (54) (2023) 20773–20803. https://doi.org/10.1016/j.ijhydene.2023.02.110

[16] R.E. Stoller, 1.11 - Primary radiation damage formation, in: R.J.M. Konings (Ed.), Comprehensive Nuclear Materials, Elsevier, Oxford, 2012, pp. 293–332. https://doi.org/10.1016/B978-0-08-056033-5.00027-6

[17] S. Reboh, M.F. Beaufort, J.F. Barbot, J. Grilhé, P.F.P. Fichtner, Orientation of H platelets under local stress in Si, Appl. Phys. Lett. 93 (2008) 022106. https://doi.org/10.1063/1.2958212

[18] S. Kirnstoetter, M. Faccinelli, C. Gspan, W. Grogger, M. Jelinek, W. Schustereder, J.G. Laven, H.-J. Schulze, P. Hadley, High dose proton implantations into silicon: a combined EBIC, SRP and TEM study, physica status solidi (c) 11 (11-12) (2014) 1545–1550. https://doi.org/10.1002/pssc.201400051

[19] H.-R. Sander, M. Hempel, Zug-druck-wechselfestigkeit und eigenschaftsänderungen von stählen nach kaltverformung mit unterschiedlicher geschwindigkeit, Archiv für das Eisenhüttenwesen 23 (7-8) (1952) 299–320. https://doi.org/10.1002/srin.195200955

[20] H. Bhadeshia, Developments in martensitic and bainitic steels: role of the shape deformation, Mater. Sci. Eng. A 378 (1-2) (2004) 34–39. https://doi.org/10.1016/j.msea.2003.10.328

[21] J. Venezuela, Q. Liu, M. Zhang, Q. Zhou, A. Atrens, The influence of hydrogen on the mechanical and fracture properties of some martensitic advanced high strength steels studied using the linearly increasing stress test, Corros. Sci. 99 (2015) 98–117. https://doi.org/10.1016/j.corsci.2015.06.038

[22] R.Z. Valiev, T.G. Langdon, Principles of equal-channel angular pressing as a processing tool for grain refinement, Prog. Mater. Sci. 51 (7) (2006) 881–981. https://doi.org/10.1016/j.pmatsci.2006.02.003

[23] C. Liang, G. Song, W. Wang, J. Zeng, In-situ observation of the multi-phase transition and microstructure evolution of 22MnB5 steel, Metall. Mater. Trans. B 55 (5) (2024) 3866–3878. https://doi.org/10.1007/s11663-024-03223-x

[24] J.F. Ziegler, M.D. Ziegler, J.P. Biersack, SRIM–the stopping and range of ions in matter (2010), Nucl. Instrum. Methods Phys. Res. Sect. B 268 (11-12) (2010) 1818–1823. https://doi.org/10.1016/j.nimb.2010.02.091

[25] R.E. Stoller, M.B. Toloczko, G.S. Was, A.G. Certain, S. Dwaraknath, F.A. Garner, On the use of SRIM for computing radiation damage exposure, Nucl. Instrum. Methods Phys. Res. Sect. B 310 (2013) 75–80. https://doi.org/10.1016/j.nimb.2013.05.008

[26] L.A. Giannuzzi, J.L. Drown, S.R. Brown, R.B. Irwin, F.A. Stevie, Applications of the FIB lift-out technique for TEM specimen preparation, Microsc. Res. Tech. 41 (4) (1998) 285–290. https://doi.org/10.1002/(sici)1097-0029(19980515)41:4<285::aid-jemt1>3.0.co;2-q

[27] R.F. Egerton, Electron energy-loss spectroscopy in the electron microscope, Springer Science & Business Media, 2011. https://doi.org/10.1007/978-1-4419-9583-4

[28] L. Zhu, Z. Gu, H. Xu, et al., Modeling of microstructure evolution in 22MnB5 steel during hot stamping, J. Iron. Steel Res. Int. 21 (2014) 197–201. https://doi.org/10.1016/S1006-706X(14)60030-3

[29] M. Okayasu, T. Fujiwara, Hydrogen embrittlement characteristics of hot-stamped 22MnB5 steel, Int. J. Hydrogen Energy 46 (37) (2021) 19657–19669. Materials and membranes for hydrogen separation/purification processes. https://doi.org/10.1016/j.ijhydene.2021.03.092

[30] M.A. Tunes, D. Parkison, Y. Huang, M.R. Chancey, S.C. Vogel, V.K. Mehta, M.A. Torrez, E.P. Luther, J.A. Valdez, Y. Wang, et al., Challenges in developing materials for microreactors: a case-study of yttrium dihydride in extreme conditions, Acta Mater. 280 (2024) 120333. https://doi.org/10.1016/j.actamat.2024.120333

[31] F.R.N. Nabarro, Rafting in superalloys, Metall. Mater. Trans. A 27 (1996) 513–530. https://doi.org/10.1007/BF02648942

[32] J.Y. Buffiere, M. Ignat, A dislocation based criterion for the raft formation in nickel-based superalloys single crystals, Acta Metall. Mater. 43 (1995) 1791–1797. https://doi.org/10.1016/0956-7151(94)00432-H

[33] Z. Yu, X. Wang, F. Yang, Z. Yue, J.C.M. Li, Review of γ' rafting behavior in nickel-based superalloys: crystal plasticity and phase-field simulation, Crystals 10 (2020) 1095. https://doi.org/10.3390/CRYST10121095

[34] L.S. Darken, R.P. Smith, Behavior of hydrogen in steel during and after immersion in acid, Corrosion 5 (1) (1949) 1–16. https://doi.org/10.5006/0010-9312-5.1.1

[35] R.A. Oriani, The diffusion and trapping of hydrogen in steel, Acta Metall. 18 (1) (1970) 147–157. https://doi.org/10.1016/0001-6160(70)90078-7

[36] P. Lang, M. Rath, E. Kozeschnik, P.E.J. Rivera-Diaz-del Castillo, Modelling the influence of austenitisation temperature on hydrogen trapping in Nb containing martensitic steels, Scr. Mater. 101 (2015) 60–63. https://doi.org/10.1016/j.scriptamat.2015.01.019

[37] M.A. Stopher, P. Lang, E. Kozeschnik, P.E.J. Rivera-Diaz-del Castillo, Modelling hydrogen migration and trapping in steels, Mater. Des. 106 (2016) 205–215. https://doi.org/10.1016/j.matdes.2016.05.051

[38] S. Zamberger, P. Lang, E. Kozeschnik, Modeling the influence of atomic traps on H diffusion and solubility in steel, in: Proc. 11th Int. Seminar on Numerical Analysis of Weldability, 2016, pp. 423–433. https://doi.org/10.1016/j.commatsci.2015.11.014

[39] D. Zügner, S. Zamberger, N. Yigit, G. Rupprechter, E. Kozeschnik, Thermal desorption spectra of H in an Fe–C–Nb alloy evaluated by diffusion simulation, Steel Res. Int. 91 (12) (2020) 2000240. https://doi.org/10.1002/srin.202000240

[40] J.H. Evans, Simulations of the effects of 2-D interstitial diffusion on void lattice formation during irradiation, Philos. Mag. 86 (2006) 173–188. https://doi.org/10.1080/14786430500380134

[41] J.H. Evans, Comments on the role of 1-D and 2-D self-interstitial atom transport mechanisms in void- and bubble-lattice formation in cubic metals, Philos Mag. Lett. 87 (2007) 575–580. https://doi.org/10.1080/09500830701393148

[42] R.W. Harrison, G. Greaves, J.A. Hinks, S.E. Donnelly, Engineering self-organising helium bubble lattices in tungsten, Sci. Rep. 7 (1) (2017) 7724. https://doi.org/10.1038/s41598-017-07711-w

[43] M. Koyama, M. Rohwerder, C.C. Tasan, A. Bashir, E. Akiyama, K. Takai, D. Raabe, K. Tsuzaki, Recent progress in microstructural hydrogen mapping in steels: quantification, kinetic analysis, and multi-scale characterisation, Mater. Sci. Technol. 33 (13) (2017) 1481–1496. https://doi.org/10.1080/02670836.2017.1299276

[44] W.H. Johnson, On some remarkable changes produced in iron and steel by the action of hydrogen and acids, Nature 11 (281) (1875) 393–393. https://doi.org/10.1038/011393a0

[45] W.H. Johnson, II. On some remarkable changes produced in iron and steel by the action of hydrogen and acids, Proc. R. Soc. London 23 (156-163) (1875) 168–179. https://doi.org/10.1038/011393a0

[46] M.W. Thompson, Defects and Radiation Damage in Metals, Cambridge University Press, London, London, 1969. https://doi.org/10.1088/0031-9112/20/12/008

[47] S.E. Donnelly, J.H. Evans, Fundamental aspects of inert gases in solids, 279, Springer Science & Business Media, 1991. https://doi.org/10.1007/978-1-4899-3680-6

[48] J.H. Evans, Observations of a regular void array in high purity molybdenum irradiated with 2 MeV nitrogen ions, Nature 229 (5284) (1971) 403–404. https://doi.org/10.1038/229403a0

[49] J.H. Evans, Void and bubble lattice formation in molybdenum: a mechanism based on two-dimensional self-interstitial diffusion, J. Nucl. Mater. 119 (2-3) (1983) 180–188. https://doi.org/10.1016/0022-3115(83)90195-2

[50] R.W. Harrison, G. Greaves, J.A. Hinks, S.E. Donnelly, A study of the effect of helium concentration and displacement damage on the microstructure of helium ion irradiated tungsten, J. Nucl. Mater. 495 (2017) 492–503. https://doi.org/10.1016/j.jnucmat.2017.08.033

[51] R.W. Harrison, S. Ebert, J.A. Hinks, S.E. Donnelly, Damage microstructure evolution of helium ion irradiated SiC under fusion relevant temperatures, J. Eur. Ceram. Soc. 38 (11) (2018) 3718–3726. https://doi.org/10.1016/j.jeurceramsoc.2018.04.060

[52] R.W. Harrison, On the use of ion beams to emulate the neutron irradiation behaviour of tungsten, Vacuum 160 (2019) 355–370. https://doi.org/10.1016/j.vacuum.2018.11.050

[53] H. Schroeder, P.F.P. Fichtner, On the coarsening mechanisms of helium bubbles–Ostwald ripening versus migration and coalescence, J. Nucl. Mater. 179 (1991) 1007–1010. https://doi.org/10.1016/0022-3115(91)90261-5

[54] M.J. Zehetbauer, Effects of non-equilibrium vacancies on strengthening, Key Eng. Mater. 97 (1995) 287–306. https://doi.org/10.4028/www.scientific.net/KEM.97-98.287

[55] D. Guedes, A. Oudriss, S. Frappart, G. Courlit, S. Cohendoz, P. Girault, J. Creus, J. Bouhattate, A. Metsue, F. Thebault, et al., The influence of hydrostatic stress states on the hydrogen solubility in martensitic steels, Scr. Mater. 84 (2014) 23–26. https://doi.org/10.1016/j.scriptamat.2014.04.006

[56] S.M. Myers, M.I. Baskes, H.K. Birnbaum, J.W. Corbett, G.G. DeLeo, S.K. Estreicher, E.E. Haller, P. Jena, N.M. Johnson, R. Kirchheim, et al., Hydrogen interactions with

defects in crystalline solids, Rev. Mod. Phys. 64 (2) (1992) 559. https://doi.org/10.1103/revmodphys.64.559
[57] K. Ito, Y. Tanaka, K. Tsutsui, H. Sawada, Analysis of grain-boundary segregation of hydrogen in BCC-Fe polycrystals via a nano-polycrystalline grain-boundary model, Comput. Mater. Sci 225 (2023) 112196. https://doi.org/10.1016/j.commatsci.2023.112196
[58] M. Faccinelli, S. Kirnstoetter, M. Jelinek, T. Wuebben, J.G. Laven, H.-J. Schulze, P. Hadley, Diffusion of hydrogen in proton implanted silicon: Dependence on the hydrogen concentration, (2016). https://doi.org/10.1557/proc-507-679
[59] C.D. Beachem, A new model for hydrogen-assisted cracking (hydrogen "embrittlement"), Metall. Mater. Trans. B 3 (1972) 441–455. https://doi.org/10.1007/bf02642048
[60] S. Lynch, Hydrogen embrittlement phenomena and mechanisms, Corros. Rev. 30 (3-4) (2012) 105–123. https://doi.org/10.1515/corrrev-2012-0502
[61] L.B. Pfeil, The effect of occluded hydrogen on the tensile strength of iron, Proc. R. Soc. London. Ser. A Containing Pap. Math. Phys. Charact. 112 (760) (1926) 182–195. https://doi.org/10.1098/rspa.1926.0103
[62] A.R. Troiano, The role of hydrogen and other interstitials in the mechanical behavior of metals, Trans. ASM 52 (1960) 54–81. https://doi.org/10.1007/s13632-016-0319-4
[63] K. Sugita, M. Mizuno, H. Araki, Y. Shirai, T. Omura, K. Tomatsu, Y. Sakiyama, Review of positron lifetime studies of lattice defects formed during tensile deformation in a hydrogen environment, ISIJ Int. 61 (2021) 1056–1063. https://doi.org/10.2355/isijinternational.ISIJINT-2020-550
[64] M. Nagumo, Hydrogen related failure of steels–a new aspect, Mater. Sci. Technol. 20 (8) (2004) 940–950. https://doi.org/10.1179/026708304225019687
[65] M. Nagumo, et al., Fundamentals of Hydrogen Embrittlement, 921, Springer, 2016. https://doi.org/10.1007/978-981-10-0161-1_6
[66] M. Nagumo, K. Takai, The predominant role of strain-induced vacancies in hydrogen embrittlement of steels: overview, Acta Mater. 165 (2019) 722–733. https://doi.org/10.1016/j.actamat.2018.12.013